Nuclear Mathematical and Computational Sciences: A Century in Review, A Century Anew
Gatlinburg, Tennessee, April 6-11, 2003, on CD-ROM, American Nuclear Society, LaGrange Park, IL (2003)

STEADY STATE ANALYSIS OF MULTIGROUP DIFFUSION AND SPN METHODS IN AN MSLB-LIKE SITUATION USING THE CRONOS CODE SYSTEM

Jean C Ragusa
CEA-Saclay
Direction de l'Energie Nucléaire
Service d'Etudes des Réacteurs et de Modélisations Avancées
91 191 Gif sur Yvette, FRANCE
jean.ragusa@cea.fr

ABSTRACT

An MSLB-like situation, for which the flux is highly disturbed, is computed with the multigroup Diffusion, SPN, and SN methods in 2- and 3-D. Cross-sections are generated using parallel task distribution, are homogenized over the entire assembly and collapsed in various energy meshes. Our analysis shows that the homogenization/collapse/equivalence process used to generate the homogeneous multigroup cross-sections performs poorly for the SPN and the SN methods, and that many energy groups are needed to achieve convergence, whereas B1-leakage theory leads to a satisfactory diffusion coefficient for the diffusion approximation. If SPN or SN methods are to be used in 2-, 3-D, few groups routine calculations, an improved equivalence formalism is needed in order to obtain adequate few-group cross-sections.

Key Words: SPN methods, cross-section generation, equivalence

1. INTRODUCTION

Simplified P_N equations applied to 3-D nuclear core computations have become quite popular in the recent years [1], [2]. The multi-D SP_N equations can be derived either heuristically from the spherical harmonic or P_N equations written in 1-D, in which the odd angular flux moments were previously eliminated, or following an asymptotic derivations as shown in [3], [4]. In 1-D, SP_N equations are obviously identical to the P_N equations. It is also well known that in multi-D, the SP_N solution does not converge towards the P_N solution, and is therefore referred to as a "simplified transport" or also a "super diffusion" method.
The purpose of the paper is to analyze quantitatively the behavior of the multigroup SP_N solution in the case of steep flux variations as encountered during a Main Steam Line Break (MSLB) and to compare these results with the customary diffusion solutions. A preliminary study regarding the feedback cross-section generation is included. In the work reported here, steady state multigroup SP_N calculations are performed for a 3D French PWR, using quarter assembly homogeneous modeling of the core; it is intended to extend this analysis to heterogeneous 17 pins x 17 pins assemblies.

In Sec.2, we will briefly recall the SP_N equations (with anisotropic scattering source) and mention the formulation used to solve them in the CRONOS code system.

In Sec. 3, the generation of assembly cross-sections will be presented: a new parallel methodology will be implemented to drastically reduce the computational burden associated with feedback cross-sections dedicated to accident analysis. Equivalent reflector constants will also be computed in many energy meshes, for several simplified transport operators.
Sec 4. will be dedicated to the presentation of the 1300 MWe PWR modeled for this study. The transient MSLB calculation will be performed, leading to high peaked fluxes and T/H feedback that will be used for all subsequent steady-state calculations. Sec. 5 will be dedicated to the 3-D diffusion and SP_N computations and comparisons. 2-D diffusion, SP_N, and S_N computations will be presented in Sec. 6.

2. SPN EQUATIONS

The SP_N equations are written with anisotropic scattering as follows:

$$\begin{cases} t_0\Sigma_{r,0}\Psi_0 + h_1\vec{\nabla}\cdot\vec{\Psi}_1 = t_0 Q_0 \\ \cdots \\ h_n\vec{\nabla}\cdot\vec{\Psi}_{n-1} + t_n\Sigma_{r,n}\Psi_n + h_{n+1}\vec{\nabla}\cdot\vec{\Psi}_{n+1} = t_n Q_n \\ h_{n+1}\vec{\nabla}\Psi_n + t_{n+1}\Sigma_{r,n+1}\vec{\Psi}_{n+1} + h_{n+2}\vec{\nabla}\Psi_{n+2} = t_{n+1}\vec{Q}_{n+1} \\ \cdots \\ h_N\vec{\nabla}\Psi_{N-1} + t_N\Sigma_{r,N}\vec{\Psi}_N = t_N\vec{Q}_N \end{cases}$$

with the removal cross-section and the anisotropic scattering and fission sources defined as follows:

$$\Sigma_{r,n} = \Sigma_t - \Sigma_{s,n}$$

$$Q_n = \sum_{g'\neq g}\Sigma_{s,n}^{g'g}\Psi_n^{g'} + d_{n0}\tfrac{1}{l}c^g\sum_{g'}\nu\Sigma_f^{g'}\Psi_0^{g'}$$

coefficients h_i and t_i can be chosen appropriately to simplify matrices expressions.

Transport corrections can be applied to this system, for any n. Therefore, when using n-corrected scattering cross-sections, the source term Q_l vanishes for $l>n$. For the purpose of this work, the diagonal transport correction and the extended transport corrections [5] were implemented in CRONOS.
It is customary to combine the SP_N equations two by two, which lead to diffusion like coupled equations. A diffusion solver can therefore be easily turned into an SP_N solver by looping on the even flux harmonics. In CRONOS, the mixed-dual variational formulation utilized for the multigroup diffusion equation has been extended to the SP_N equations. In the diffusion framework, a mixed dual formulation leads to the concomitant resolution of the flux and the current. This translates into both even scalar unknowns and odd vector unknowns being solved for in the SP_N mixed dual formulation [1].

3. CROSS SECTION GENERATION

3.1 Parameterized cross-section library parallel generation

Cross-sections utilized in the CRONOS code are arranged as a hierarchal library of elementary APOLLO-2 [6] computations, performed at each state point. A state point is defined as a set of values for each parameter or multiplet M defined as:

$$M = (\cdots, V_i^{P_k}, \cdots)$$

where V is the i^{th} value of the k^{th} parameter ($1 \le i \le I_k$, $1 \le k \le N$, with N, number of parameters and I_k, number of values for the k^{th} parameter).

Typically, a CRONOS cross-sections library is parameterized according to the following: burn-up, moderator temperature and density, fuel temperature, boron concentration. For each computational mesh in the nuclear core, a linear interpolation in the R^N hypercube is performed to compute the feedback cross-sections. In the case of a MSLB accident, the following parameterization was used, leading to 50 596 elementary lattice computations (cf. Table I).

Table I. Chosen Parameters for the feedback cross-section generation

Parameter	Number of values	Values
fuel temperature, °C	7	200, 435.37, 761.14, 1028.6 , 1505.0, 1872.9, 2071.9
moderator temperature , °C	2	200 , 300
moderator density, g/cm^3	13	.350, 0.375, 0.400, 0.4375, 0.475, 0.500, 0.550, 0.600, 0.650, 0.700, 0.750, 0.800, 0.900
Boron concentration, ppm	2	0, 300
Burn-Up, MWd/t	16 (UOX) 25 (UOX-Gd_2O_3)	The nominal isotopic fuel depletion is performed on a finer grid; the feedback cross-sections are computed on a subset of the depletion grid

In the current feedback cross-section library generation routine, imbedded loops on the different parameters are used, and all state points are computed sequentially. This scheme is modified here to make use of the obvious bijection between the elementary calculations number and the state point value sets (multiplet M). The various imbedded loops are replaced with a unique loop, which renders the cross-section generation easy to parallelize. Message Passing Interface (MPI) is used as communication protocol. The MSLB cross-section library, which would have required several days of sequential CPU time, was obtained, using the parallelized routine, in 4 hrs (7 hrs resp.) for the UOX (resp. UOX-Gd_2O_3) assemblies using 13 processors of the CEA SMP Compaq machine (Digital EV68 833 MHz processors).

The elementary APOLLO-2 computations are performed with the following state-of-the-art PWR production calculation scheme:

- 172 group microscopic cross-section library based on JEF2.2 (CEA93.v6 library)
- CP multi-cell 1/8 assembly computation with all 39 fuel pins individually represented (6 rings per pin)
- Depletion and self-shielding performed for every fuel mesh
- B1 homogenous leakage calculation [7]

Spatial homogenization and energy condensation are performed for either the entire assembly or pin-by-pin (pin-by-pin results were not complete to be included in this paper), using 2, 4, 8 and 20 macro-energy groups (see Appendix A). Super-homogenization theory is used during the

condense/collapse stage, and SPH factors [8] are included in the output libraries. In the case of homogenous condensation, flux weighting leads in all SPH being equal to 1, which is obvious since the equivalence is performed on an homogenous infinite medium. Using the so-called Selengut equivalence for the homogenous condensation, SPH factors other than one are obtained (in this latter case, the SPH factors can be related to the widely used discontinuity factors).

3.2 Reflector constants

Reflector constants are generated using the multigroup beta equivalence [9] method. For many energy groups (>8), the method fails to converge as is, and basic linesearch and backtracking techniques are used to obtain a more stable scheme. Figure 1 shows the power and the fluxes for groups 1, and 20 (in 20 macro-groups case) obtained for a simple 1-D geometry computed with either albedo boundary conditions or with an equivalent reflector mesh using vacuum boundary condition (or zero-flux in the case of the diffusion operator). Nevertheless, the method is found to be highly sensitive to the initial guess. Such drawbacks lead us to believe that the equivalent reflector problem should be tackled with a more robust approach. Since reflector constants result from an equivalence theory, a set of reflector constants has to be computed for every low-order operator that is to be utilized in the 3-D core computation (i.e. diffusion/SP_N operator, for each energy macrogroup).

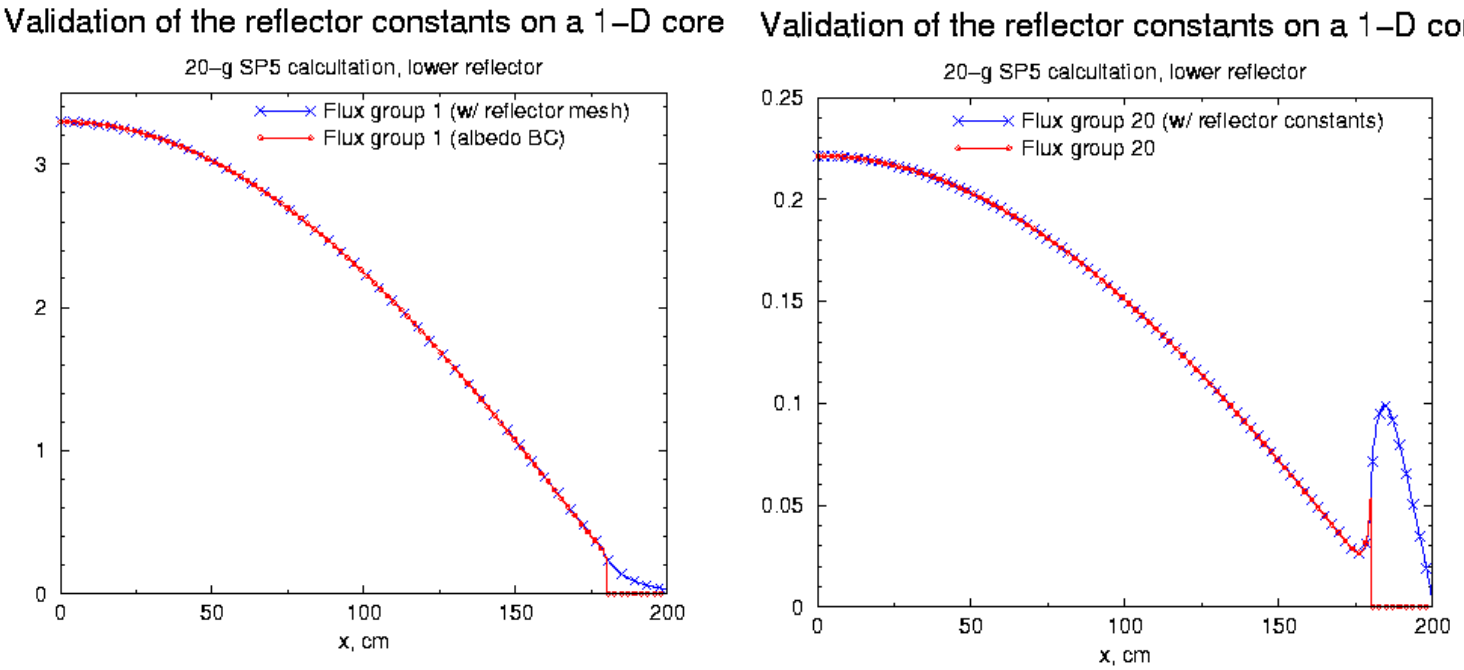

Figure 1. Validation of the reflector constants on a 1-D core

4. DESCRIPTION OF THE PWR CORE MODELED AND DETERMINATION OF THE MSLB-LIKE 3-D T/H CONDITIONS

A 1300 MW_e (3800 MW_{th}) French PWR was chosen for this study. The 193 assemblies are loaded into the 3-batch core: 121 UOX assemblies with 4%w/o, and 72 UOX-Gd_2O_3 assemblies for reactivity control. A radial loading map, with the UOX/UOX-Gd assemblies, control rod bank positions, and batch number is shown on Fig. 2. According to the SSAR, MSLB accidents for such a core are analyzed at the following conditions:

- End of Cycle (EOC)
- Hot Zero Power (HZP)
- all rods inserted except one (the control rod stuck out is shown on Fig 2)
- penalty Xe distribution.

Primary and secondary loop transient calculations are performed using CATHARE, and 3-D core coupled thermal-hydraulics (T/H) / neutronics transient calculations are performed using CRONOS and FLICA with CATHARE's boundary conditions. Usually, semi-empirical inlet mixing matrices are utilized for the core inlet conditions to couple the system code with the core code; the neutronics operator utilized is customarily the 2-group diffusion (with diffusion coefficients from a B1 homogenous lattice computation). Assemblies are treated as one T/H channel (with sub-channel analysis), and 4 neutronics meshes. 400 sec of coupled transient were computed on a Dec-α 600 MHz in about 11 days.

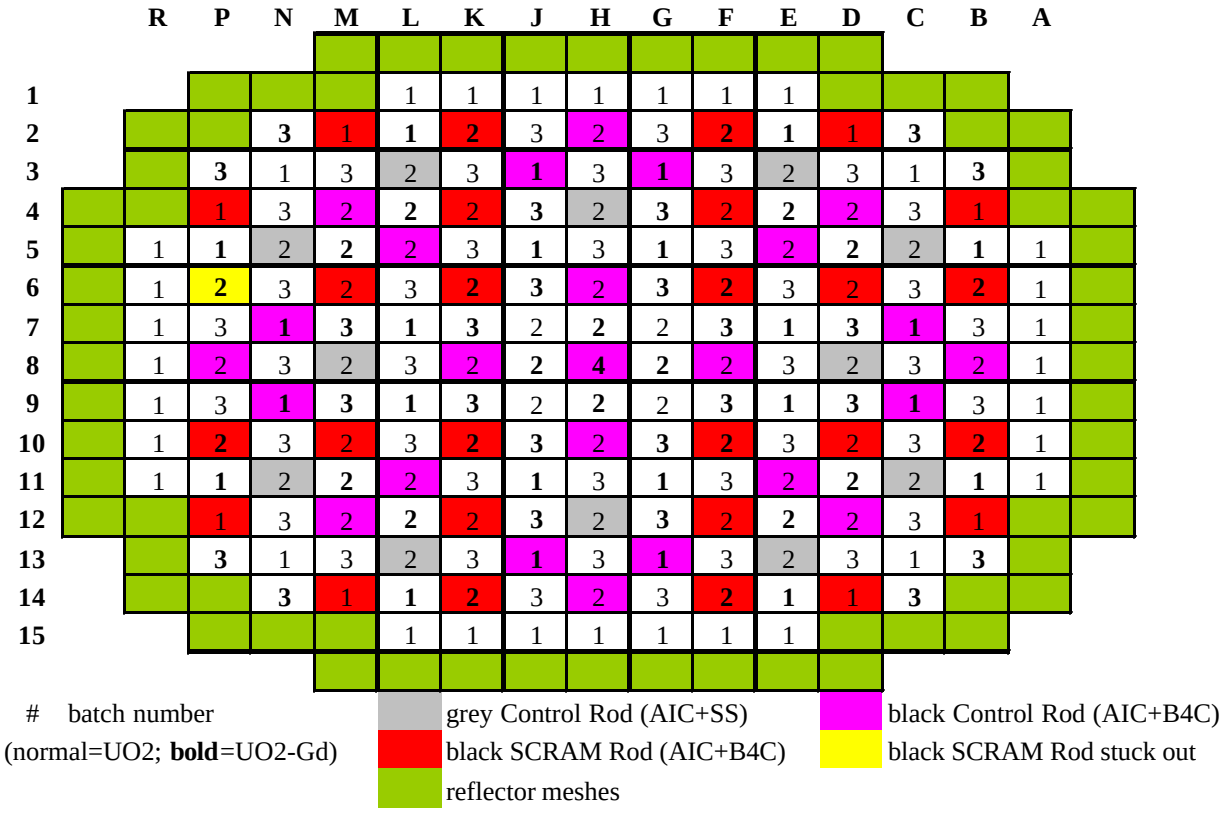

Figure 2. Core loading pattern and rod positions.

Fig. 3 shows the system boundary conditions computed with CATHARE (intact and broken legs temperatures, core boron concentration, core inlet and outlet pressures) as well as the power level computed with CRONOS / FLICA.

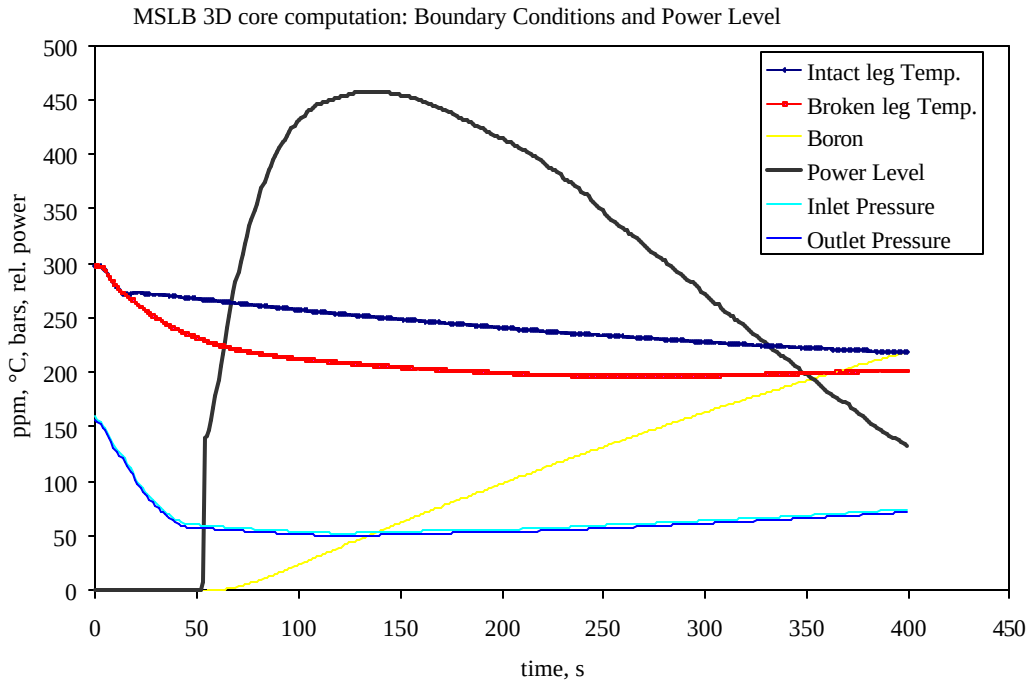

Figure 3. 3-D core MSLB computation

Diffusion theory lacking accuracy in voided regions, and in regions with steep flux gradient, it is expected that a MSLB accident, with localized significant void and high peaking factor, will reveal some of the deficiencies of diffusion theory. Our goal is to carry on diffusion/SP_N comparisons in order to reveal some discrepancies.

Nevertheless, performing such a transient computation by replacing the classical 2-group diffusion operator with a multigroup SP_N operator could be tedious and unsatisfactory. It is more fruitful to focus our attention for the diffusion/SP_N analysis at steady state, with fixed T/H conditions from the transient. The fixed T/H conditions are chosen in order to lead to the most disturbed flux in the core. This happens to be around 120-130 sec in the transient, when the pressure is at the lowest, and the void fraction at the highest. Table II summarizes some of the results obtained for MSLB calculation at 120 sec, and Fig. 4 & 5 present the radial power and the axial power distributions obtained with 2g- diffusion.

Table II. 3-D core MSLB calculation relevant figures

Thermal-hydraulics			Neutronics	
	Minimum value	Maximum value	K_{eff}	0.98 913
T_{fuel}, °C	242.09	1110.87	Axial-Offset, %	-41.23
T_{mod}, °C	221.83	264.81	F_{xy}	10.63
D_{mod}, g/cm^3	0.508	0.842	F_z	2.32
α, %	0.	35.85	F_{xyz}	24.12

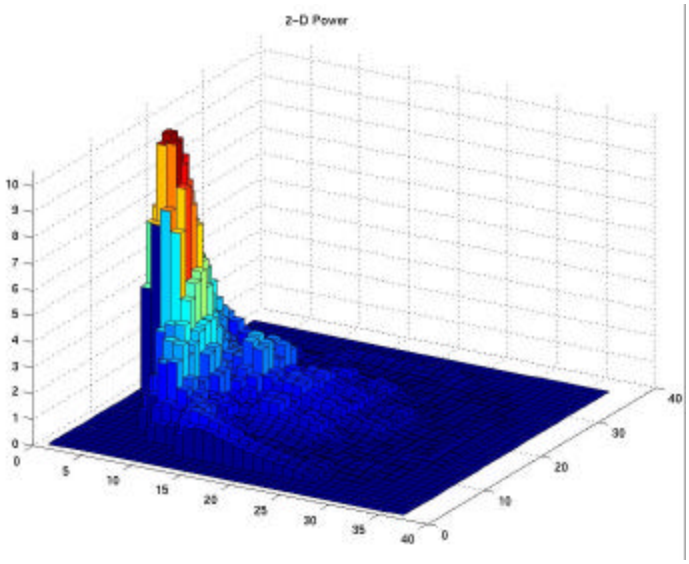

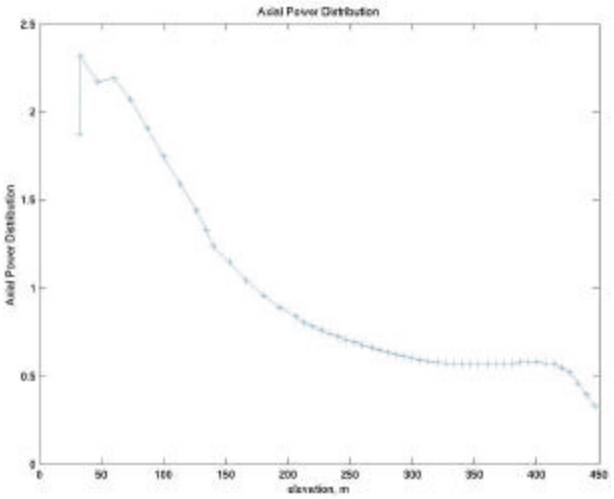

Figures 4 & 5. Radial and axial power distributions (3-D core MSLB computation)

5. 3-D DIFFUSION / SP_N COMPARISONS

The 3-D core presented in the previous section was computed with the fixed T/H conditions obtained during the MSLB computation. The computational mesh utilized was a quarter assembly of height 13 cm. Raviart-Thomas-Nedelec finite elements are used [10], with quadratic degree in the 3 directions (RTN_2 elements). Gauss-Legendre quadrature is used for the numerical integration (superconvergence properties).

Figures 6 & 7 show the eigenvalues and the quarter assembly peaking factors obtained for various multigroup simplified transport operators, with different collision anisotropy order: SP_NP_M (where N is the flux harmonics order and M is the scattering anisotropy order). Three diffusion operators were also used; they differ by the diffusion coefficient D utilized:

- Diffusion_tot uses $1/3\Sigma_{total}$ for D,
- Diffusion_tra uses $1/3\Sigma_{transport}$ for D,
- Diffusion_B1 uses leakage/B^2 for D (B_1 theory)

On figures 6 & 7, the red line symbolizes our 3-D "reference" calculation (20 groups, SP5 with P2 corrected cross-sections). The reference computation took 150 000 sec CPU time and 1 300 Mwords of memory on a Dec-α EV6 450 MHz.

Discussion (regarding figures 6 & 7 and table III):

- Scattering Anisotropy order: P0 correction for the scattering cross-section is an obvious improvement over P0 cross-section. When increasing the anisotropy order, the transport correction effect weakens, since the values of the cross-sections themselves diminish, but there is still a discrepancy between P1 and P2 cross-sections. We note that a P1 corrected development accounts for most of the P2 development.
- Angular Flux Harmonics Development: There is about 4 pcm discrepancy in the eigenvalue and 0.2% discrepancy in the power peaking factor (ppf) between the scattering converged SP5 calculation (SP5P5) and the scattering converged calculation (SP3P3c).
- Energy groups: simplified transport operators show a slow energy convergence for the 3-D computations (it was previously observed that SP_N methods converge for 16-20 energy groups [11]). The matter will be further discussed in the next section.
- Diffusion/SP_N comparison:
  - diffusion calculations using the diffusion coefficient from B1 leakage theory are very stable with respect to the number of energy groups and are in good agreement with the 20-g SP5P2c reference calculation.
  - Diffusion calculations using $1/3\Sigma_{total}$ or $1/3\Sigma_{transport}$ for D show a behavior similar to the SPN computations. Indeed, diffusion calculations using $1/3\Sigma_{total}$ should be the same as the SP1P0 computations and diffusion calculations using $1/3\Sigma_{transport}$ should be the same as the SP1P0c computation since the equations are strictly the same. This is not the case because of the use of equivalence theory in the generation of the core and reflector cross-sections. We verified that most of the discrepancies were due to the equivalent reflector constants.

Table III. 3-D core SP_N comparisons (8 groups): Anisotropic scattering order effect and flux development order effect

Simplified Transport Operator	Scattering Cross-section Anisotropy (c = transport corrected)										
	P0	P0c	P1	P1c	P2	P2c	P3	P3c	P4	P4c	P5
	Eigenvalues Comparison (errors in pcm, reference in bold)										
SP1	-3925,5	299,6	0	**0,990 695**							
SP3	-3899,9	194,3	25,5	2,5	-1,2	-1	0	**0,993 131**			
SP5	-3899,7	184,6	26,2	2,1	-0,9	-0,8	0	0	0	0	**0,993 093**
	Quarter Assembly Peaking Factors Comparison (errors in %, reference in bold)										
SP1	-281,77	25,61	0,01	**23,12**							
SP3	-258,20	17,59	1,10	0,06	-0,04	-0,04	0,00	**25,72**			
SP5	-258,98	17,57	1,13	0,06	-0,03	-0,03	0,00	0,00	0,00	0,00	**25,67**

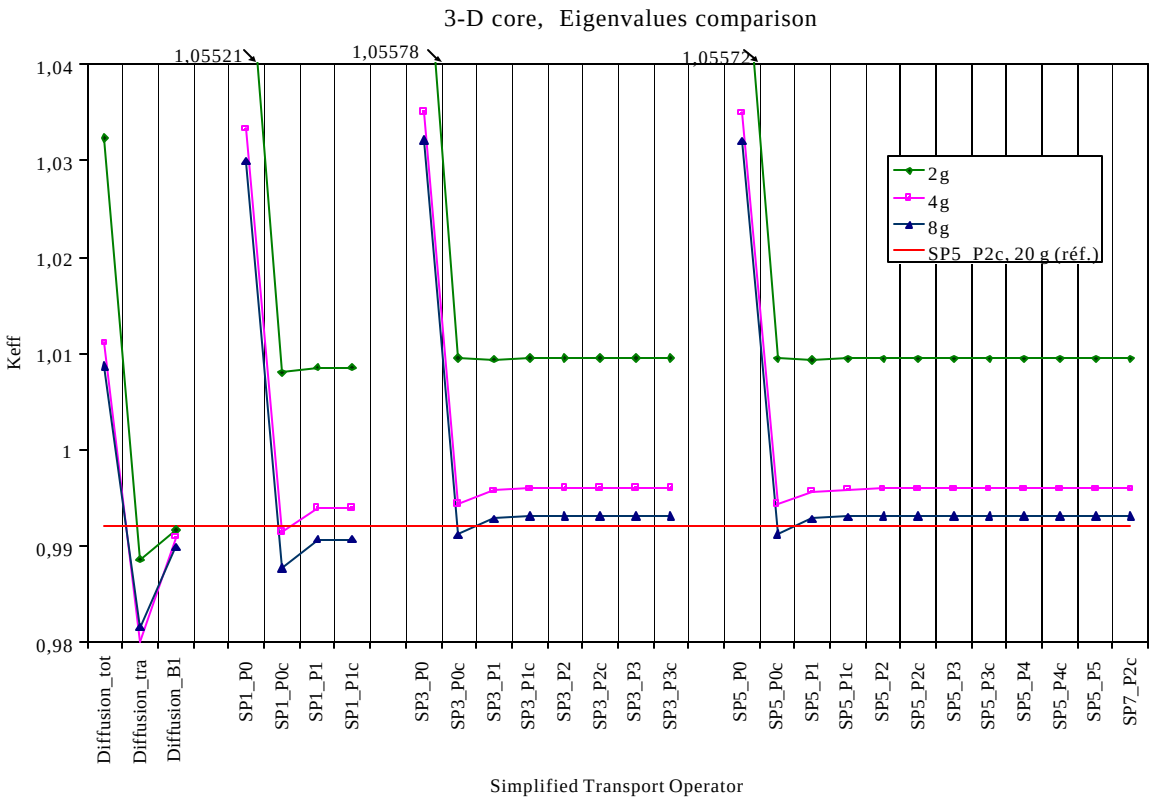

Figure 6. Diffusion / SPN eigenvalues comparisons

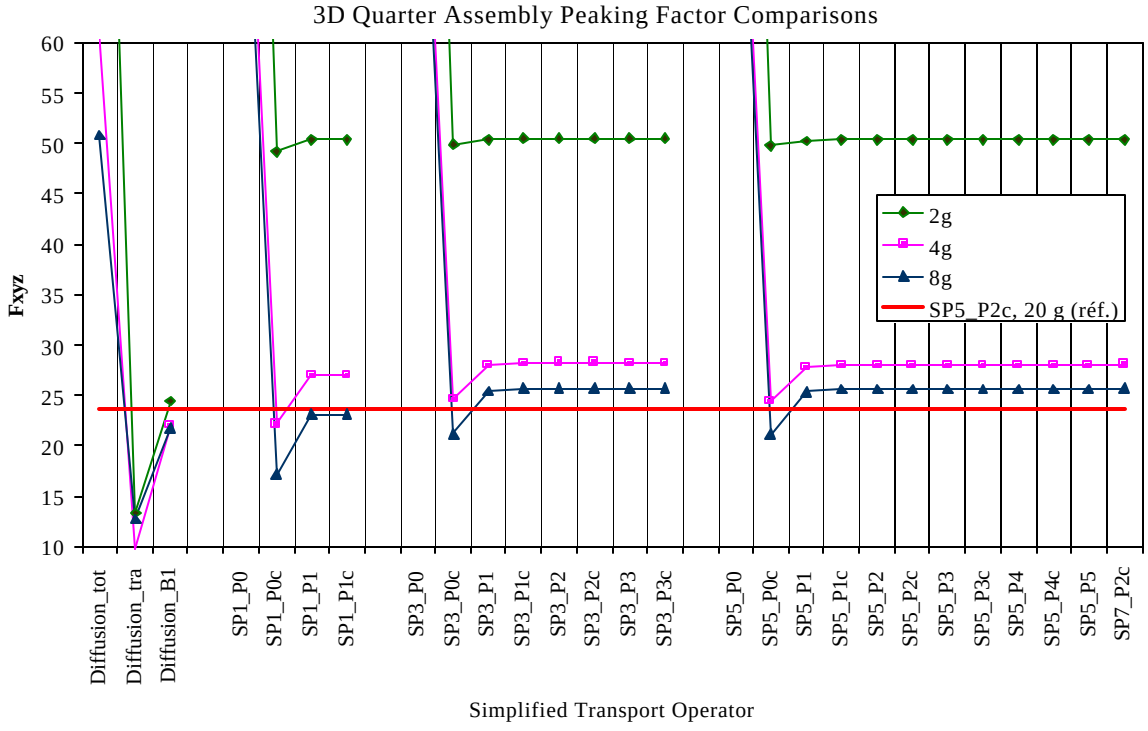

Figure 7. Diffusion / SPN power peaking factors comparisons

5. 2-D comparisons

In order to further analyze the diffusion/SP_N behavior observed in the previous section, 2-D computations using albedo boundary condition are carried on. Replacing the reflector and vacuum boundary condition with the 1-D albedo used in the reflector constants generation gets rid of the operator-dependent reflector cross-sections. 2-D geometry also allows for S_N computations. Figures 8 & 9 show the eigenvalues and the 2-D p.p.f. obtained for diffusion, SP_N and S_N calculations (very similar plots were obtained when repeating the computations without SPH factors).

Discussion:

- the same behavior for the transport (SP_N and S_N) calculations is observed:
  - P1c corrected cross-sections are needed for convergence on the scattering terms
  - SP3 approximation suffices for the flux development
  - Convergence on the energy groups is slow
- this time, diffusion calculations using $1/3\Sigma_{total}$ are exactly the same as the SP1P0 computations and diffusion calculations using $1/3\Sigma_{transport}$ are the same as the SP1P0c computations
- diffusion theory using the B1-homogeneous leakage model for the diffusion coefficient D is in good agreement with the much finer transport calculations (20-g S16 or 20-g SP9P2c).
- The use or not of SPH factors does not modify our findings.

The SP_N computations showed the same behavior with respect to the energy discretization (with or without equivalence theory). During the homogenization-condensation stage, cross-sections are collapsed on the whole assembly, on fewer energy groups. The last step of the homogenization-condensation stage is the equivalence process. During the equivalence process, we impose that the low order transport assembly calculation (homogeneous assembly, few energy groups, diffusion or SPN operator) preserve the reaction rates from the high order transport assembly calculation (heterogeneous mesh, many groups, CP method). When equivalence theory is used on an infinite homogenous medium, the resulting flux is flat and isotropic. According to the normalization used, SPH factors are either equal to one or not, depending on the preservation of the macrogroup flux or the use Selengut normalization. In any case, information regarding neutron leakage is no longer present at that stage.

1. When the low order transport operator is the diffusion operator, the Laplacian vanishes (homogeneous case medium) and the coefficient is a "free" parameter. D is collapsed like a cross-section by preserving leakage rate (DB^2).
2. When the low order transport operator is the SPN or SN operator, the advection term vanishes. Scattering cross-sections (σ_l, $l>0$) are undetermined (just the D was undetermined in the case of the diffusion operator). In our calculation scheme, the scattering cross-sections (σ_l, $l>0$) are collapsed using the scalar flux. Some attempts at collapsing them with higher flux moments have been unsuccessful [12], but we believe that the equivalence theory used does not suffice when collapsing the cross-sections into a homogeneous assembly with fewer groups.

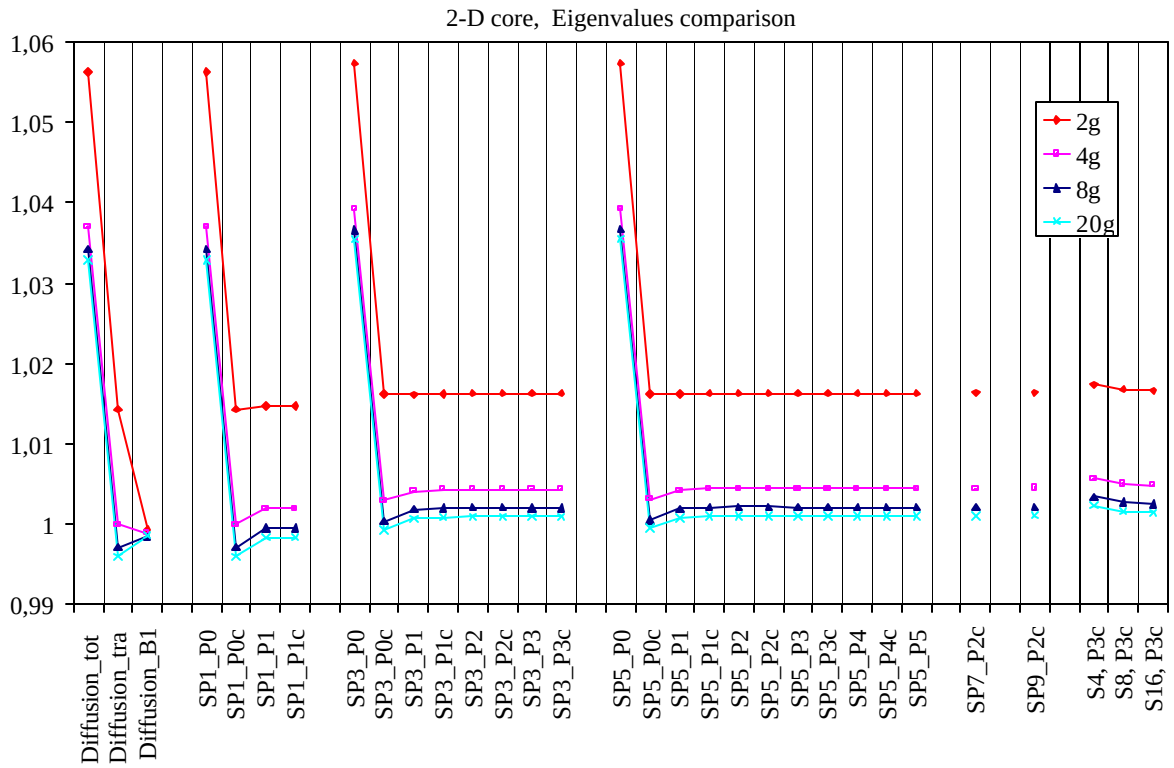

Figure 8. Diffusion / SPN eigenvalues comparisons

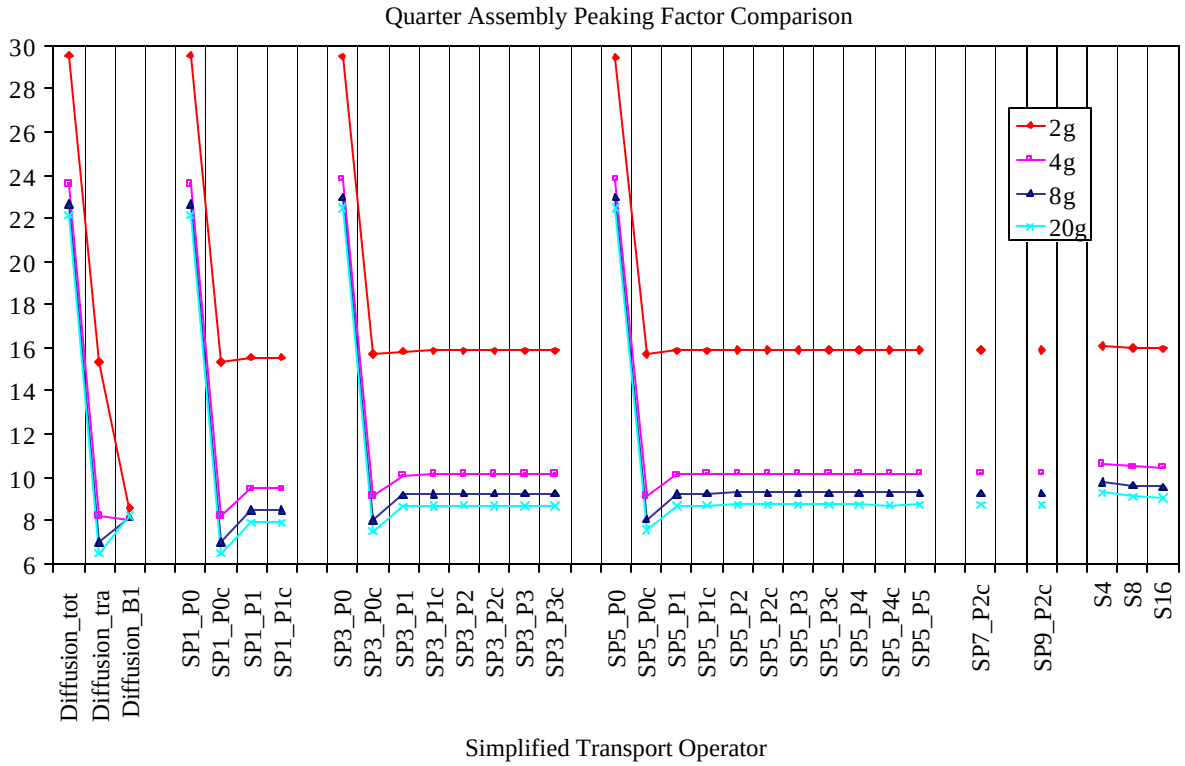

Figure 9. Diffusion / SPN ppf comparisons

Finally, it is observed that an increase in the number of energy groups leads to more consistent or converged results. This is expected, since, in the limit of 172 groups, equivalence is no longer necessary (or in other words, collapsed cross-sections depend less on the weighting function as the number of energy groups increases).

6. CONCLUSIONS

An MSLB-like problem was computed in 2 and 3-D with several simplified transport operators and compared to the diffusion solutions. Diffusion theory using $1/3\Sigma_{total}$ or $1/3\Sigma_{transport}$ for D gives erroneous results compared to the 20-g SP5 computation in 3-D or compared to the 20-g S16 computation in 2-D. Diffusion theory using the B1-leakage model for D shows good agreement with many-group high order transport results. Few-group transport computations do not give the correct answer. Equivalence theory in infinite homogenous medium will be further analyzed to determine its impact on the scattering cross-sections.
Heterogeneous (i.e. pin-by-pin) computations will be presented in a subsequent paper.

REFERENCES

1. J.-J. Lautard, D. Schneider, A.-M. Baudron, "Mixed Dual Methods for Neutronic Reactor Core Calculations in the CRONOS System", *Proceeding of the ANS Mathematics and Computation International Conference*, Madrid, Spain, Sept. 1999
2. C. H. Lee, T. J. Downar, "Application of a Two-Level Acceleration Method to the Pin-by-Pin Multigroup SP_3 Approximation", *Trans. AM. Nucl. Soc.*, **85**, 243 (2001).
3. G. C. Pomraning, "Asymptotoc and Variational Derivation of the Simplified PN Equations", Ann. Nucl. Energy, Vol 20, No 9, pp. 623-637
4. E. W. Larsen, "Asymptotic Derivation of the Simplified PN Equations", *International Conference on Mathematical Methods and Supercomputing in Nuclear Applications*, Karlsruhe, Germany, April 1993
5. G. I. Bell, G. E. Hansen, H. A. Sandmeier, "Multitable Treatments of Anisotropic Scattering in SN Multigroup Transport Calculations", *Nucl. Sci. Eng.*, **28**, 376-383 (1967).
6. S. Loubière, R. Sanchez, M. Coste, A. Hébert, Z. Stankovski, C. Van der Gucht, I. Zmijarevic, "APOLLO2 Twelve Years Later", *Proceeding of the ANS Mathematics and Computation International Conference*, Madrid, Spain, Sept. 1999
7. P. Benoist, "Homogenization Theory in Reactor Lattices", CEA-N-2471 (1986) (publicly available)
8. A. Hébert, G. Mathonnière, "Development of a Third Generation SPH Method for the Homogenization of a Pressurized Water Reactor Assembly", *Nucl. Sci. Eng.*, **115**, 129 (1993).
9. E. Richebois, C. Fedon-Magnaud, P. Magat, G. Mathonnière, S. Mengelle, A. Nicolas, "Determination of Multigroup and Multi-operator Reflector Constants: Application to a Power Reactor Transport Calculation", *International Conference on the Physics of Nuclear Science and Technology*, Long Island, New-York 1998.
10. J.C. Nedelec, "A new family of mixed finite elements in R3", Numerische Mathematik, Vol. **50**, p.57-81, 1986
11. E. Richebois, "Calcul de Coeur REP en transport 3D", CEA-R-5935

12. P Magat, “Analyse des techniques d’homogénéisation spatiale et énergétique dans la resolution de l’équation du transport des neutrons dans les réacteurs nucléaires”, PhD thesis, Université Aix-Marseille I, April 1997 .

APPENDIX A

Energy group	Energy upper bound (MeV)
1	$2{,}0000.10^{1}$
2	$6{,}2500.10^{-7}$

Energy group	Energy upper bound (MeV)
1	$2{,}0000.10^{1}$
2	$9{,}0718.10^{-1}$
3	5,0045.10-3
4	$6{,}2500.10^{-7}$

Energy group	Energy upper bound (MeV)
1	$2{,}0000\ 10^{1}$
2	$1{,}3533\ 10^{0}$
3	$1{,}8315\ 10^{-1}$
4	$2{,}0346\ 10^{-3}$
5	$5{,}5595.10^{-5}$
6	$4{,}0000.10^{-6}$
7	$6{,}2500.10^{-7}$
8	$1{,}3400.10^{-7}$

Energy group	Energy upper bound (MeV)
1	$2{,}0000\ 10^{1}$
2	$4{,}4932.10^{0}$
3	$2{,}2313.10^{0}$
4	$1{,}3533.10^{0}$
5	$4{,}9787.10^{-1}$
6	$1{,}8315\ .10^{-1}$
7	$2{,}4788.10^{-2}$
8	$6{,}7379.10^{-2}$
9	$9{,}1188.10^{-3}$
10	$2{,}0346.10^{-2}$
11	$4{,}5399.10^{-4}$
12	$5{,}5595.10^{-5}$
13	$4{,}000.10^{-6}$
14	$6{,}25.10^{-7}$
15	$3{,}50.10^{-7}$
16	$2{,}20.10^{-7}$
17	$1{,}34.10^{-7}$
18	$7{,}7.10^{-8}$
19	$3{,}0.10^{-8}$
20	$1{,}0.10^{-8}$

Table A. Energy cut-offs used in Cronos-2